Available online at www.sciencedirect.com
ScienceDirect
Journal of Power Sources 162 (2006) 1395–1400
JOURNAL OF POWER SOURCES
www.elsevier.com/locate/jpowsour

Short communication

Simulation of charge–discharge cycling of lithium-ion batteries under low-earth-orbit conditions

Jong-Won Lee, Yogesh K. Anguchamy, Branko N. Popov *

Center for Electrochemical Engineering, Department of Chemical Engineering, University of South Carolina, Columbia, SC 29208, USA

Received 20 July 2006; accepted 21 July 2006
Available online 1 September 2006

Abstract

Charge–discharge behavior of SONY 18650 lithium-ion batteries for aerospace applications was simulated under low-earth-orbit (LEO) conditions, by using a first-principles based mathematical model. The model determines the capacity fade on the basis of the irreversible loss of active lithium ions due to electrolyte reduction. The capacity fade during LEO cycling was studied for 5 years of continuous operation with 20% depth of discharge as a function of the cycling parameters such as the end of charge voltage and the charging rate.

Keywords: Lithium-ion battery; Capacity fade simulation; Aerospace application; Low-earth-orbit

1. Introduction

Rechargeable lithium-ion batteries have much higher energy density, both volumetric and gravimetric, compared with conventional alkaline and nickel–hydrogen batteries, and have been considered as alternative power sources to space-qualified nickel–hydrogen systems for orbiter applications, ranging from 'geostationary-earth-orbit' (GEO) to 'low-earth-orbit' (LEO) [1].

Since the batteries are used only when the satellite is hidden from the sun by the earth during eclipse period, the requirements strongly depend on the orbit condition [2–5]. A satellite in LEO (within 1000 km from the earth) uses its batteries far more often than a GEO satellite (within 3.6×10^4 km from the earth) that is rarely in the earth's shadow cone. Thus, the depth of discharge (DOD) should be limited to low levels of 20–40%, in order not to overstress the batteries. Typically, the batteries in a LEO satellite require a life time over 5 years, i.e. the cycle life exceeding up to 3×10^4 cycles.

While lithium-ion technology has been successfully used in GEO satellites [6], the long-term cycle life under LEO conditions has not been validated yet. There are only limited long-term test data available on lithium-ion batteries under LEO conditions [4,5]. Therefore, model-based estimation of cycle life and capacity will demonstrate the applicability of lithium-ion batteries for orbiter power sources. The present work involves simulation of charge–discharge cycling of lithium-ion batteries for LEO applications using a first-principles based model previously developed by us at USC [7]. In particular, the effects of the cycling parameters such as DOD, end of charge voltage (EOCV) and charging rate on performance of the battery were investigated under LEO conditions.

2. Simulation model and cycling protocols

A mathematical model based on porous electrode theory, concentrated solution theory, Ohm's law, and Butler–Volmer intercalation kinetics was developed by us previously which predicts the capacity fade of a lithium-ion cell [7,8]. In the model, it was assumed that the capacity fade results from the irreversible loss of active lithium ions due to electrolyte reduction on the anode surface. When the carbon anode is polarized more cathodically than the reversible potential for parasitic reaction during the charging process, the electrolyte solvent (specifically, ethylene carbonate) is reduced to insoluble salts, resulting in formation of a resistive surface film [9–12]. The increase of the surface film resistance with cycling was also taken into account

* Corresponding author. Tel.: +1 803 777 7314; fax: +1 803 777 8265.
E-mail address: popov@engr.sc.edu (B.N. Popov).

0378-7753/$ – see front matter © 2006 Elsevier B.V. All rights reserved.
doi:10.1016/j.jpowsour.2006.07.045

Nomenclature

a_i	specific surface area of porous electrode (cm^{-1})
C_{Li^+}	lithium ion concentration in the electrolyte ($mol\,cm^{-3}$)
C_i^{Li}	lithium concentration in the electrode ($mol\,cm^{-3}$)
C_i^{Li-S}	lithium concentration at the electrode/electrolyte interface ($mol\,cm^{-3}$)
C_i^{max}	maximum lithium concentration in the electrode ($mol\,cm^{-3}$)
D_i	lithium diffusivity in the electrode ($cm^2\,s^{-1}$)
F	Faraday constant ($C\,mol^{-1}$)
I_{app}	applied current (A)
I_i	electric current (A)
J_i	total Faradaic current density across the electrode/electrolyte interface ($A\,cm^{-2}$)
J_i^{Li}	current density for intercalation/deintercalation reactions ($A\,cm^{-2}$)
J_{i0}^{Li}	exchange current density for intercalation/deintercalation reactions ($A\,cm^{-2}$)
J_s^{Li}	current density for parasitic reaction ($A\,cm^{-2}$)
J_{s0}^{Li}	exchange current density for parasitic reaction ($A\,cm^{-2}$)
k_i	rate constant for intercalation/deintercalation reactions ($A\,m^{2.5}\,C^{-1}\,mol^{-0.5}$)
Q_s	loss of active lithium ions (Ah)
r_i	radial coordinate (cm)
R	gas constant ($J\,mol^{-1}\,K^{-1}$)
R_i	radius of electrode particles (cm)
R_s	resistance of newly formed surface film (Ω)
R_i^f	total film resistance (Ω)
S_i	superficial surface area (cm^2)
t	time (s)
T	absolute temperature (K)
T_s	total parasitic reaction time (s)
U	local equilibrium potential (V)

Greek letters

α	transfer coefficient of electrochemical reaction
δ	surface film thickness (cm)
ε	volume fraction of a solid phase
ϕ	potential of a phase (V)
η	overpotential for electrochemical reaction (V)
κ	conductivity of newly formed surface film ($S\,cm^{-1}$)

Subscripts or superscripts

1	solid phase
f	film on the particle surfaces
i	negative or positive electrode
n	negative electrode (anode)
N	cycle number
p	positive electrode (cathode)
s	parasitic reaction

Table 1
Key parameters used in the simulation model

Parameter	Anode	Cathode
Lithium diffusivity, D_i ($cm^2\,s^{-1}$)	3.8×10^{-10}	1.0×10^{-9}
Rate constant for lithium intercalation/deintercalation, k_i ($A\,m^{2.5}\,C^{-1}\,mol^{-0.5}$)	1×10^{-6}	1×10^{-6}
Reversible potential for parasitic reaction, U_s^{OCP} (V vs. Li^+/Li)	0.38	–
Exchange current density for parasitic reaction, J_{s0}^{Li} ($A\,cm^{-2}$)	2.5×10^{-12}	–
Conductivity of surface film, κ ($S\,cm^{-1}$)	5.0×10^{-8}	–

in calculation of the charge–discharge curves. No parasitic reaction was assumed to occur on the cathode surface. The mathematical model is fully described in Appendix A.

In this work, the simulations were performed based on the experimental data obtained from a SONY 18650 (G8) lithium-ion cell which consists of carbon anode and $LiCo_xMn_yNi_zO_2$ cathode. The discharge capacity of the cell was experimentally determined to be 2.293 Ah at 1.126 A, and this value was used for calculation of charging and discharging currents.

The previous model was modified to simulate the charge–discharge cycling under LEO conditions as follows [6]: the duration of LEO was assumed to be 90 min, i.e. 35 min eclipse and 55 min sunshine. The cell was galvanostatically discharged for 35 min at a rate calculated using the required DOD value. Next, the cell was galvanostatically charged, until EOCV was reached, at a rate that is 1.1 times the rate necessary to return the discharged capacity. Finally, the cell was potentiostatically charged at EOCV until a total of 55 min of charge was achieved. The cycle life was defined as the cycle number at which the end of discharge voltage (EODV) dropped below 3.0 V [4,5]. For capacity check, the cell was discharged at a *C*/2 rate to 3.0 V, and then it was charged by using a conventional protocol of constant current (CC)–constant voltage (CV), viz. a *C*/5 rate to 4.2 V with a 50 mA cut-off current. All the simulations were run at 25 °C. The key parameters used in the model are listed in Table 1.

3. Results and discussion

Fig. 1(a) shows typical potential and current profiles computed for the first LEO cycle. The simulations were run at different DOD values of 20–40% for EOCV of 4.05 V. Under LEO conditions, the orbit duration (charge and discharge times) remains constant during cycling, and thus the model controls DOD by controlling the charging and discharging currents. It is seen that the larger the DOD value is, the lower is the EODV value.

Fig. 1(b) presents the plots of EODV of the cell against cycle number measured experimentally and simulated theoretically. The measurements and simulations were performed at 20 and 40% DOD values for EOCV of 4.05 V. As a result of the irreversible loss of lithium ions due to the parasitic reaction during the charging process, the lithium content (state of charge) in the anode at the beginning of discharge decreases gradually with cycling (see Eq. (A.19)). In order to maintain the required

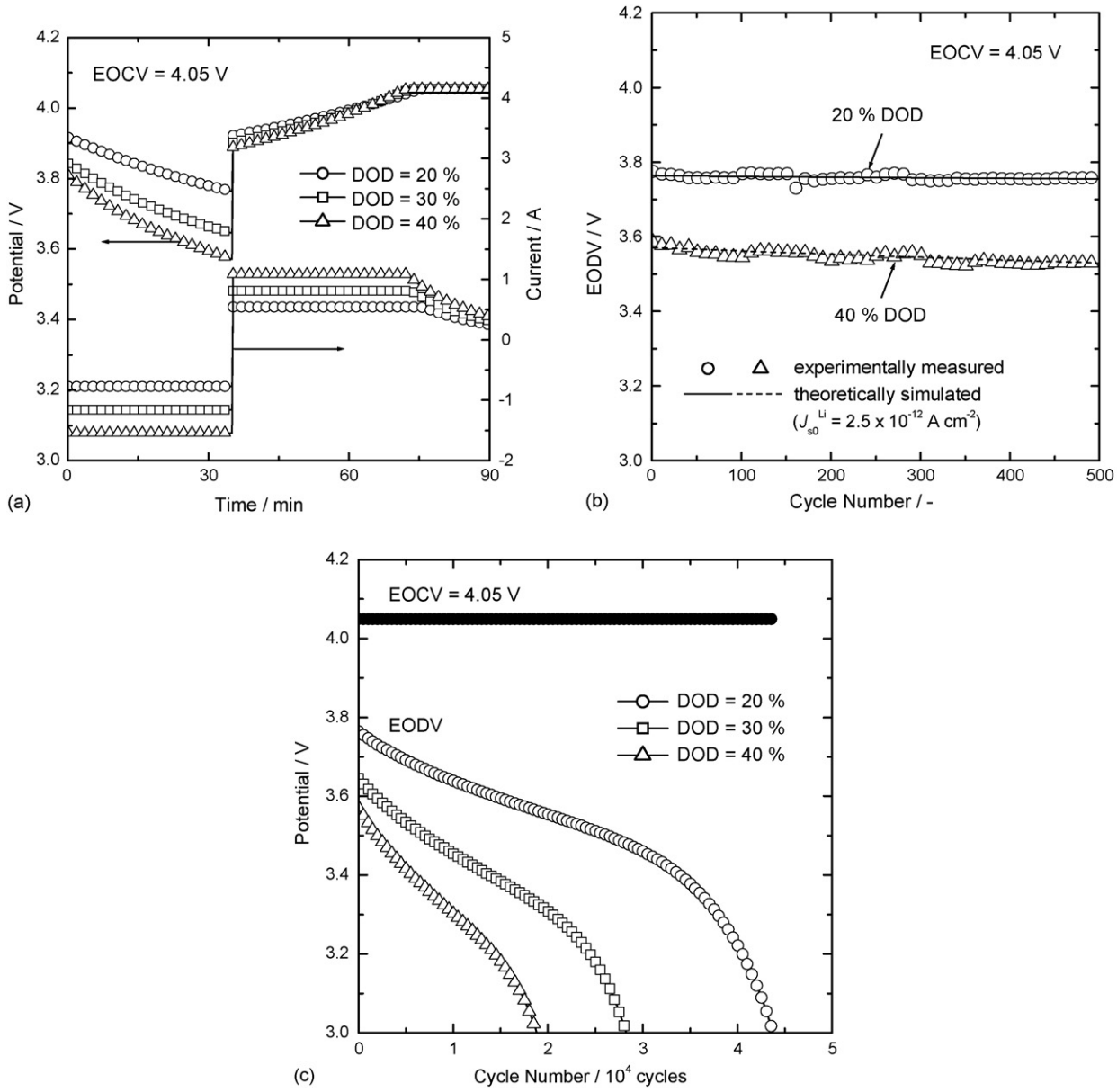

Fig. 1. (a) Potential and current profiles simulated for the first LEO cycle, (b) the measured and (c) simulated EODV values as a function of cycle number. The simulations were performed with $J_{s0}^{Li} = 2.5 \times 10^{-12}$ A cm^{-2} for EOCV of 4.05 V.

DOD, the lithium content in the anode at the end of discharge decreases, causing the EODV of the anode to rise with cycling. Consequently, the cell discharges to lower potential, as the LEO cycling progresses.

In the model, the parasitic reaction rate on the anode surface was assumed to be given by the Tafel equation (Eq. (A.14)). The exchange current density for parasitic reaction J_{s0}^{Li} depends on the electrolyte composition and electrode structures in the specific battery, and was used as an adjustable parameter in the simulation. As shown in Fig. 1(b), it was found that EODV calculated with $J_{s0}^{Li} = 2.5 \times 10^{-12}$ A cm^{-2} gives the best fit to the experimental data for both DOD values.

In Fig. 1(c), the simulated values of EODV were plotted as a function of cycle number for EOCV of 4.05 V to determine the cycle life. From this figure, the cycle life was predicted to be approximately 4.4, 2.8 and 1.9×10^4 for the DOD values of 20, 30 and 40%, respectively. The simulations performed using various cycling parameters indicated that only the LEO cycling with 20% DOD in the EOCV range of 3.85–4.05 V yields the cycle life greater than 3×10^4 cycles which meets the requirement for LEO applications.

Recently, Fellner et al. [4] reported the experimental test data on the long-term cycling of lithium-ion cells used for LEO spacecrafts up to 9×10^3 cycles. They projected the cycle life of about 2.7×10^4 cycles from a linear extrapolation of EODV toward 3.0 V at 40% DOD. However, the simulation results in this study demonstrate that the plot of EODV versus cycle number deviates significantly from linearity, as the LEO cycling proceeds. The cycle life predicted from a linear extrapolation by Fellner et al. has been overestimated.

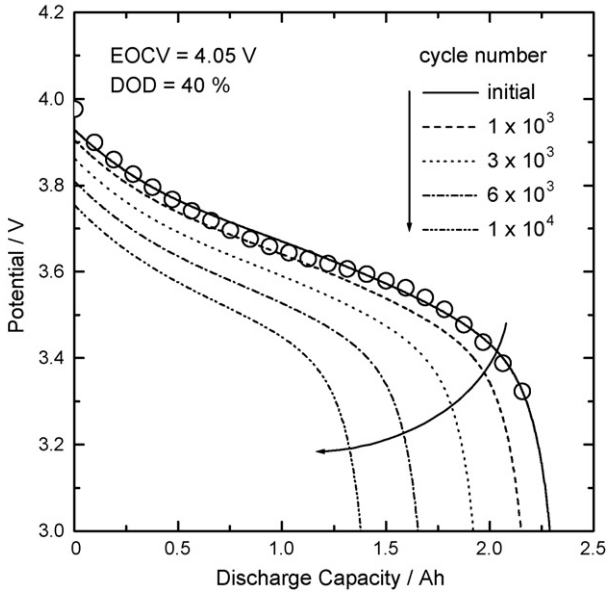

Fig. 2. Galvanostatic discharge curves simulated at different cycle numbers at the rate of *C*/2. The simulations were run using EOCV of 4.05 V and DOD of 40%. The initial discharge curve measured experimentally is denoted as open circle in the figure.

Fig. 2 presents the discharge curves simulated at different cycle numbers. The capacity check was done using a rate of *C*/2. The LEO cycling was run at EOCV of 4.05 V and to DOD of 40%. For comparison, the initial discharge curve measured experimentally is also shown in Fig. 2. As shown in this figure a good agreement between the experimental and simulated curves is observed. The potential plateau of the simulated discharge curves decreases gradually with cycling, which is attributed to the continuous increase in the resistance of the surface film. The simulation predicts a decrease of the discharge capacity from the initial value of 2.293 to 1.38 Ah after 1×10^4 cycles.

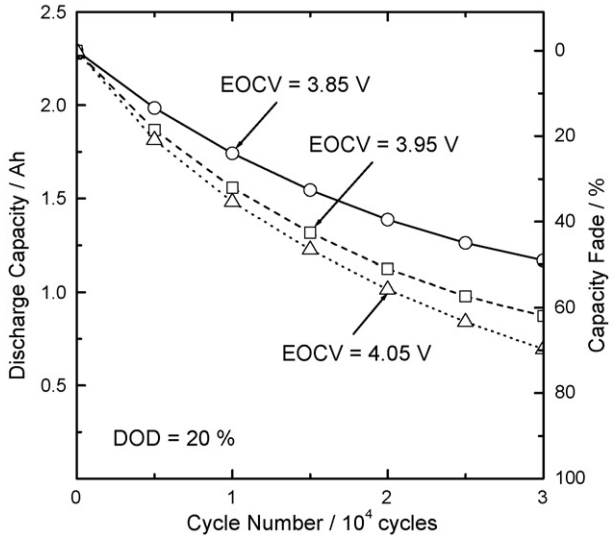

Fig. 3. Effect of EOCV on the capacity fade during LEO cycling with 20% DOD.

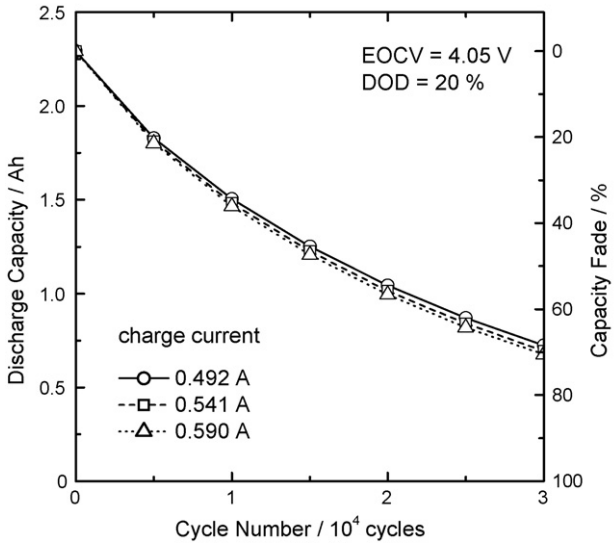

Fig. 4. Discharge capacity and capacity fade as a function of cycle number simulated at various charging rates. The simulations were performed with EOCV of 4.05 V and DOD of 20%.

Fig. 3 summarizes the projected capacity fades of the cell for 5 years of continuous operation with 20% DOD and EOCV in the range of 3.85–4.05 V. In the model, the parasitic reaction rate and thus the loss of active lithium ions depend on the overpotential for parasitic reaction η_s on the anode surface. According to Eq. (A.14) in Appendix A, EOCV increases the overpotential η_s during the charging process, thereby accelerating the solvent reduction reaction. This results in the increased capacity fade at higher EOCV as presented in Fig. 3.

Fig. 4 shows the discharge capacities simulated at different charging currents. The simulations were run using EOCV of

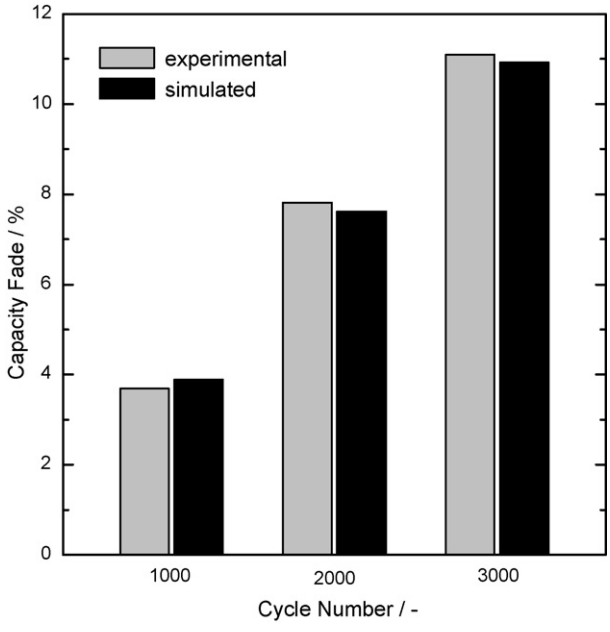

Fig. 5. Comparison of the capacity fades of lithium-ion batteries simulated theoretically and determined experimentally [6].

4.05 V and DOD of 20%. The charging currents of 0.492, 0.541 and 0.590 A correspond to the rates of 0.22, 0.24 and 0.26 C, respectively. As the charging current increases from 0.492 to 0.590 A, the capacity fade increases due to the increase of the overpotential for the parasitic reaction. Also, the cycle life was predicted to decrease from 45,774 to 42,373 cycles with increasing the charging current, which suggests that the use of low charging rate is recommended to accomplish a long-term for LEO cycling.

Fig. 5 compares the simulated capacity fades with those measured experimentally during LEO cycling with EOCV of 3.95 V and DOD of 20% [6]. The simulated capacity fades at different cycle numbers are in good agreement with the experimental values as shown in Fig. 5. In our laboratory the experimental long-term test of lithium-ion cells is in progress, and the results will be presented for comparison with the simulation data in the following paper.

4. Conclusions

A first-principles based mathematical model was used to simulate charge–discharge cycling of SONY 18650 lithium-ion batteries for aerospace applications under LEO conditions. Since the orbit duration remains constant during LEO cycling, the model controls DOD by controlling the charging and discharging currents. The capacity fade was calculated on the basis of the irreversible loss of active lithium ions due to electrolyte reduction. For 5 years of continuous operation with a shallow depth of discharge of 20%, the capacity fade during LEO cycling was studied as a function of EOCV and charging rate. The simulated values of capacity fade were found to be in good agreement with the experimental values at different cycle numbers.

Acknowledgement

Financial support provided by NASA John H. Glenn Research Center is acknowledged gratefully.

Appendix A

Assuming that the active electrode materials are composed of uniform spherical particles with a radius of R_i, the diffusion of lithium in the solid phase is described by Fick's second law for a sphere

$$\frac{\partial C_i^{Li}}{\partial t} = \frac{\tilde{D}_i}{(r_i)^2}\frac{\partial}{\partial r_i}\left(r_i^2\frac{\partial C_i^{Li}}{\partial r_i}\right) \tag{A.1}$$

The initial condition (IC) and the boundary conditions (BC) for galvanostatic charging/discharging are as follows:

$$\text{IC}: \quad C_i^{Li} = C_{i0}^{Li}, \quad \text{for } 0 \le r_i \le R_i \text{ at } t = 0 \tag{A.2}$$

$$\text{BC}: \quad \frac{\partial C_i^{Li}}{\partial r_i} = 0, \quad \text{for } r_i = 0 \text{ at } t > 0 \tag{A.3}$$

$$\text{BC}: \quad \tilde{D}_i\frac{\partial C_i^{Li}}{\partial r_i} = -\frac{J_i^{Li}}{F}, \quad \text{for } r_i = R_i \text{ at } t > 0 \tag{A.4}$$

with

$$J_i^{Li} = -\frac{I_i}{S_i}, \quad S_i = a_i V_i, \quad a_i = \frac{3\varepsilon_i}{R_i} \tag{A.5}$$

Butler–Volmer kinetics was used to describe lithium intercalation/deintercalation

$$J_i^{Li} = J_{i0}^{Li}\left\{\exp\left(\frac{\alpha_i^a F}{RT}\eta_i\right) - \exp\left(-\frac{\alpha_i^c F}{RT}\eta_i\right)\right\} \tag{A.6}$$

with

$$J_{i0}^{Li} = k_i(C_i^{max} - C_i^{Li-S})^{\alpha_i^a}(C_i^{Li-S})^{\alpha_i^c}(C_{Li^+})^{\alpha_i^c},$$
$$\eta_i = \phi_i^1 - U_i^{OCP} - J_i S_i R_i^f \tag{A.7}$$

In Eq. (A.7), it was assumed that the variation of liquid phase potential along the current path is negligible. The discharge curves of the anode and cathode were measured separately at a *C*/20 rate in a three-electrode electrochemical cell with the lithium reference and counter electrodes, and then the functional expressions of U_i^{OCP} were obtained by the polynomial regression analysis of the experimental discharge curves. The following condition was used to determine the current decay in the potentiostatic charging step:

$$\phi_p^1 - \phi_n^1 = \text{EOCV} \tag{A.8}$$

Eqs. (A.1)–(A.4) were transformed into dimensionless form

$$\frac{\partial \bar{C}_i^{Li}}{\partial \bar{t}} = \frac{1}{\bar{r}_i^2}\frac{\partial}{\partial \bar{r}_i}\left(\bar{r}_i^2\frac{\partial \bar{C}_i^{Li}}{\partial \bar{r}_i}\right) \tag{A.9}$$

$$\text{IC}: \quad \bar{C}_i^{Li} = \bar{C}_{i0}^{Li}, \quad \text{for } 0 \le \bar{r} \le \bar{R}_i \text{ at } \bar{t} = 0 \tag{A.10}$$

$$\text{BC}: \quad \frac{\partial \bar{C}_i^{Li}}{\partial \bar{r}_i} = 0, \quad \text{for } \bar{r} = 0 \text{ at } \bar{t} > 0 \tag{A.11}$$

$$\text{BC}: \quad \frac{C_i^{max}\tilde{D}_i}{R_i}\frac{\partial \bar{C}_i^{Li}}{\partial \bar{r}_i} = -\frac{J_i^{Li}}{F}, \quad \text{for } \bar{r} = 1 \text{ at } \bar{t} > 0 \tag{A.12}$$

where

$$\bar{C}_i^{Li} = \frac{C_i^{Li}}{C_i^{max}}, \ \bar{r}_i = \frac{r_i}{R_i}, \ \bar{t} = \frac{t\tilde{D}_i}{R_i^2} \tag{A.13}$$

The parasitic reaction rate on the anode surface was assumed to be given by the Tafel equation

$$J_s^{Li} = J_{s0}^{Li}\exp\left(-\frac{\alpha_s^c n F}{RT}\eta_s\right) \tag{A.14}$$

with

$$\eta_s = \phi_n^1 - U_s^{OCP} - J_n S_n R_n^f \tag{A.15}$$

The total current density (J_n) at the anode is the sum of the intercalation/deintercalation current density (J_n^{Li}) and the parasitic reaction current density (J_s^{Li})

$$J_n = J_n^{Li} + J_s^{Li} = \frac{I_{app}}{S_n} \tag{A.16}$$

The electronic charges are completely consumed by the intercalation/deintercalation of lithium at the cathode

$$J_p = J_p^{Li} = \frac{I_{app}}{S_p} \tag{A.17}$$

The loss of active lithium ions was estimated using the following equation:

$$Q_s = \int_0^{T_s} J_s^{Li} S_n \, dt \tag{A.18}$$

Due to the parasitic reaction, the dimensionless lithium concentration in the anode at the beginning of discharge at cycle number $(N+1)$ is less than that at cycle number N, and it is given by

$$\bar{C}_{n0}^{Li}\Big|_{N+1} = \bar{C}_{n0}^{Li}\Big|_N - \bar{Q}_s|_N \tag{A.19}$$

where

$$\bar{Q}_s|_N = \frac{Q_s|_N}{\varepsilon_n F V_n C_n^{max}} \tag{A.20}$$

Continuous precipitation of insoluble product on the anode surface causes the resistance of the film to increase with increasing the cycle number

$$R_n^f\Big|_{N+1} = R_n^f\Big|_N + R_s|_N \tag{A.21}$$

where

$$R_s|_N = \frac{\delta_f|_N}{\kappa} \tag{A.22}$$

References

[1] M.C. Smart, B.V. Ratnakumar, L.D. Whitcanack, K.B. Chin, S. Surampudi, R. Gitzendanner, F. Puglia, J. Byers, IEEE Aerospace Electron. Sys. Mag. 19 (2004) 18–25.

[2] B.V. Ratnakumar, M.C. Smart, C.K. Huang, D. Perrone, S. Surampudi, S.G. Greenbaum, Electrochim. Acta 45 (2000) 1513–1517.

[3] R.A. Marsh, S. Vukson, S. Surampudi, B.V. Ratnakumar, M.C. Smart, M. Manzo, P.J. Dalton, J. Power Sources 97–98 (2001) 25–27.

[4] J.P. Fellner, G.J. Loeber, S.P. Vukson, C.A. Riepenhoff, J. Power Sources 119–121 (2003) 911–913.

[5] X. Wang, Y. Sone, S. Kuwajima, J. Power Sources 142 (2005) 313–322.

[6] B.I. McKissock, M.A. Manzo, T.B. Miller, C.M. Reid, W.R. Bennett, R. Gemeiner, in: Proceedings of the Third International Energy Conversion Engineering Conference, San Francisco, USA, 2005.

[7] G. Ning, B.N. Popov, J. Electrochem. Soc. 151 (2004) A1584–A1591.

[8] G. Ning, R.E. White, B.N. Popov, Electrochim. Acta 51 (2006) 2012–2022.

[9] Y.-G. Ryu, S.-I. Pyun, J. Electroanal. Chem. 433 (1997) 97–105.

[10] D. Aurbach, A. Zaban, Y. Ein-Eli, I. Weissman, O. Chusid, B. Markovsky, M. Levi, E. Levi, A. Schechter, E. Granot, J. Power Sources 68 (1997) 91–98.

[11] D. Aurbach, J. Power Sources 89 (2000) 206–218.

[12] D. Aurbach, E. Zinigrad, Y. Cohen, H. Teller, Solid State Ionics 148 (2002) 405–416.